


## Coupled-channels analysis of the $\alpha$ decay in strong electromagnetic fields

S. A. Ghinescu <sup>1,2</sup> and D. S. Delion<sup>1,3,4</sup>

<sup>1</sup>*“Horia Hulubei” National Institute of Physics and Nuclear Engineering, 30 Reactorului,  
P.O. Box MG-6, RO-077125, Bucharest-Măgurele, România*

<sup>2</sup>*Department of Physics, University of Bucharest, 405 Atomîștilor, P.O. Box MG-11, RO-077125, Bucharest-Măgurele, România*

<sup>3</sup>*Academy of Romanian Scientists, 3 Ilfov RO-050044, Bucharest, România*

<sup>4</sup>*Bioterra University, 81 Gârlei RO-013724, Bucharest, România*



(Received 28 November 2019; accepted 20 March 2020; published 10 April 2020)

We investigate the influence of a monochromatic strong laser electromagnetic field on  $\alpha$  clustering and emission, by analyzing the Fourier components of the time-dependent  $\alpha$ -core realistic potential in the Henneberger representation. It turns out that the resulting potential becomes deformed and the static component is by far dominant beyond the nuclear surface where the  $\alpha$  cluster is formed, while higher Fourier terms are important in the internal region, where the  $\alpha$ -particle probability is hindered by the Pauli principle. This fact, combined with the observation that an  $\alpha$  cluster lives much longer before its emission than the laser period, allows us the use of the stationary coupled channels approach in the system of coordinates given by the laser beam direction. We predict that the angular distribution of emitted  $\alpha$  particles becomes anisotropic due to the deformation of the  $\alpha$ -core potential induced by the laser field, even for the spherical emitter  $^{212}\text{Po}$ .

DOI: [10.1103/PhysRevC.101.044304](https://doi.org/10.1103/PhysRevC.101.044304)

### I. INTRODUCTION

Different microscopic models tried to explain the process of the  $\alpha$ -particle formation on the nuclear surface within the  $R$ -matrix theory [1] or the fission-like approach [2]. The  $\alpha$  clustering plays an important role in the structure of light nuclei [3], but at the same time it is an important tool to investigate the structure of heavy and superheavy nuclei by using  $\alpha$ -decay half-lives [4]. Recent laser facilities subatomic structures to be probed by strong electromagnetic fields [5–9]. Several papers investigated the role of laser pulses on the Coulomb barrier governing the  $\alpha$ -decay process [10–12]. In Ref. [13], a semiclassical correction to the  $\alpha$ -decay rate in an oscillating electromagnetic field is obtained. The relative change in the  $\alpha$ -decay rate is calculated as a function of the nuclear charge,  $Q$  value, and the laser-radiation intensity. In Refs. [14,15], the discussion uses a quantum time-dependent formalism to investigate the manner in which the  $\alpha$ -decay dynamics in a spherical nucleus is modified by a linearly polarized ultraintense laser field. The wave-packet dynamics was determined for various laser intensities for continuous waves and for sequences of pulses, leading to an enhancement of the tunneling probability.

The use of the “adiabatic” or “static” approaches requires a special attention in analyzing the  $\alpha$ -particle emission in strong electromagnetic fields. On one hand, the  $\alpha$ -particle flight time is by several orders of magnitude smaller than the period of the electromagnetic oscillation period and therefore the  $\alpha$  tunneling has indeed an “adiabatic” nature. On the other hand, the  $\alpha$ -formation probability has a “quasistatic” character, due to the fact that  $\alpha$  emitters have a much longer half-life in comparison to the electromagnetic wave period

and even with respect to the time length of the laser pulse. Therefore, a preformed  $\alpha$  cluster on the nuclear surfaces detects an averaged surrounding Coulomb barrier.

In Ref. [16], we used the approximate Wentzel-Kramers-Brillouin (WKB) method to estimate the  $\alpha$ -decay half life in the Henneberger representation [17] for a sharp Coulomb barrier. The key point was the decoupling between radial and angular variables, because the kinetic term has the standard Laplacian form and the time-angular dependence is transferred to the potential term. Thus, due to a large Coulomb barrier, the semiclassical penetrability through a deformed potential is given by angular integration of each WKB radial term, depending on the angle  $\theta$  between the emitted particle and laser field.

Following our aforementioned work, many authors have exposed different parts [18–23]. Reference [18] gives an estimation of the WKB penetrability using a similar formalism as in Ref. [16], but considering the atomic electron cloud screening effects which is assumed to reduce by many orders of magnitude the laser field acting on the nucleus. In Ref. [19], the predicted penetrability enhancement is derived to be only some factor below 10 (depending on the laser parameters). The main cause for this is that only the spherical part of the static component of the laser field is taken into account. As will become abundantly clear in this paper, the paramount effect is the angular anisotropy induced by the laser field, with the spherical part playing only a small role.

Qi *et al.* [20] and Pálffy *et al.* [21] employ the adiabatic WKB approach in order to study the effects of strong laser fields on the  $\alpha$  decay process. Their reason for using this approximation is that the characteristic time of the decay (the time needed for the  $\alpha$  particle to cross the barrier) is

much shorter than the characteristic time of the laser field (its period). Treated rigorously, since quantum tunneling occurs almost instantaneously, the adiabatic approximation would lead to no effect on  $\alpha$  decay since there is no time for the laser to physically act on the barrier. This is the main reason for the discrepancy between their results and ours. The use of the Henneberger transformation is perfectly valid since it is a unitary transformation. The issue at hand is the validity of the Kramers approximation (i.e., replacing the time-dependent potential by its static component), which is dealt with below.

Reference [22] applies exactly the same formalism we used in Ref. [16] but using photon energies satisfying the condition  $\hbar\omega \gg Q_\alpha$ , where  $Q_\alpha$  is the  $Q$  value of  $\alpha$  decay. This fundamentally eliminates the issues regarding the use of the static approach to the tunneling phenomenon and retrieves qualitatively our previous results. We also mention here Ref. [23], which deals with strong electromagnetic fields acting on the  $\alpha$ -decaying nucleus but this time the fields themselves are static and the theoretical treatment is clear.

We also mention that the results in this paper together with the ones in our previous work [16] rely on a critical assumption: The laser field is continuous. At present, there is no high intensity, continuous laser field and the existing devices work in pulses that greatly affect our predictions. Namely, if one defines  $\tau_p$  as the duration of one pulse,  $n_p$  as the number of pulses in one cycle, and  $\tau_c$  as the duration of a cycle, the ‘‘beam efficiency’’  $\xi = n_p\tau_p/\tau_c$  is of the order of  $10^{-6}$ . This is the ratio between the time interval in which the nucleus is actually subject to the laser field and the total operating time of the apparatus. Hence, it is natural that no effect has been yet observed and technological advancements in the field of continuous lasers are critical in order to study the effects mentioned in this work.

We will analyze in this paper the validity of the static Kramers-Henneberger approach by using the exact coupled-channels method to solve the penetrations problem. At the same time, we will describe the  $\alpha$  formation on the nuclear surface in a realistic manner, consistent with available experimental data. The paper is organized according to the following plan. In Section II, we will shortly give theoretical details concerning the realistic  $\alpha$ -daughter potential and the coupled-channels approach for a deformed interaction; in Sec. III, we will estimate the angular distribution of the emitted  $\alpha$  particle; and in the last section, we will draw conclusions.

## II. THEORETICAL BACKGROUND

### A. Particle emission in an electromagnetic field

The time-dependent Schrödinger equation describing the relative motion of an  $\alpha$  particle inside the Coulomb barrier is given by

$$i\hbar \frac{\partial \Psi(\mathbf{R}, t)}{\partial t} = \left\{ \frac{1}{2M_\alpha} \left[ \mathbf{P} - \frac{e_{\text{eff}}}{c} \mathbf{A}(t) \right]^2 - V(\mathbf{R}) \right\} \Psi(\mathbf{R}, t), \quad (2.1)$$

where  $\mathbf{A}(t)$  is the time-dependent magnetic vector potential,  $e_{\text{eff}} = eZ_{\text{eff}} = e(2A - 4Z)/(A + 4)$  the effective charge [14] and  $V(\mathbf{r})$  the Coulomb potential. By using the unitary

Henneberger transformation [17],

$$\Omega = \exp \left[ \frac{i}{\hbar} \int_{-\infty}^t H_{\text{int}}(\tau) d\tau \right], \quad (2.2)$$

with

$$H_{\text{int}}(t) = -\frac{e_{\text{eff}}}{M_\alpha c} \mathbf{A} \mathbf{P} + \frac{e_{\text{eff}}^2}{2M_\alpha c^2} \mathbf{A}^2 \quad (2.3)$$

being the perturbation Hamiltonian, the new wave function  $\Phi = \Omega\Psi$  satisfies the following equation:

$$i\hbar \frac{\partial \Phi(\mathbf{R}, t)}{\partial t} = \left[ \frac{1}{2M_\alpha} \mathbf{P}^2 - V(\mathbf{R} - \mathbf{S}(t)) \right] \Phi(\mathbf{R}, t), \quad (2.4)$$

where we introduced the classical trajectory

$$\mathbf{S}(t) = \frac{e_{\text{eff}}}{M_\alpha c} \int_{-\infty}^t \mathbf{A}(\tau) d\tau. \quad (2.5)$$

We will consider in our analysis a linearly polarized laser beam

$$\mathbf{S}(\omega t) = \mathbf{e}_z S_0 \sin \omega t. \quad (2.6)$$

By using the relation connecting the intensity of the beam and the electric field magnitude [24], the amplitude of the incident beam can be written

$$S_0 = Z_{\text{eff}} \frac{\sqrt{4\pi \hbar \alpha I}}{M_\alpha \omega^2} \sim 8\sqrt{\frac{I}{10^{20}}} \left( \frac{100}{\hbar\omega} \right)^2 \text{ (fm)}, \quad (2.7)$$

in terms of the fine-structure constant  $\alpha$ , beam intensity  $I$  given in  $\text{W}/\text{cm}^2$ , and  $\hbar\omega$  in eV. It is useful to define the dimensionless parameter

$$D \equiv S_0/R_N \sim \sqrt{I}/\omega^2, \quad (2.8)$$

where  $R_N = 1.2A^{1/3}$  is the nuclear geometrical radius depending on the mass number  $A$  (which in the case of  $^{208}\text{Pb}$  is  $\approx 7.1$  fm).

The time-dependent potential in the new representation becomes axially deformed and it can be expanded in a Fourier basis as follows [11]:

$$V(\mathbf{R} - \mathbf{S}(t)) = \sum_{n=-\infty}^{\infty} V_n(\mathbf{R}) e^{in\omega t}, \quad (2.9)$$

where  $\omega = \frac{2\pi}{T}$  and  $\mathbf{R} \equiv (R, \theta)$ . Here,  $\theta$  is the angle between the emitted  $\alpha$  particle and the polarization direction  $z$  of the laser beam.

### B. Coupled-channels formalism

It is widely accepted that the  $\alpha$  particle is born on the nuclear surface, where the nuclear density has a smaller value [25], with some probability called the *spectroscopic factor* [2]. Starting from this region, it moves in the resulting nuclear plus Coulomb field of the daughter nucleus. The analysis of the  $\alpha$ -daughter interaction is a central issue of this field. One of the most popular methods is that of the double-folding procedure, presented in Refs. [26–28]. The double-folding potential that describes the elastic scattering of  $\alpha$  particles was extended to nuclei of medium mass number  $A \approx 50$ –120 nuclei at energies from  $\approx 13$  to 50 MeV in Ref. [29].

The double-folding procedure to estimate the  $\alpha$ -core potential is given by the following integral [30–32]:

$$V(\mathbf{R}) = \int d\mathbf{r}_D \int d\mathbf{r}_\alpha \rho_D(\mathbf{r}_D) \rho_\alpha(\mathbf{r}_\alpha) v(\mathbf{R} + \mathbf{r}_D - \mathbf{r}_\alpha), \quad (2.10)$$

where  $v$  denotes the nucleon-nucleon force and  $\rho_X$  is the nuclear densities of the daughter nucleus ( $X = D$ ) and  $\alpha$  particle ( $X = \alpha$ ). This method found much use in computing the potential between heavy ions having a Woods-Saxon shape for their densities. In our case, the density of the daughter nucleus is given by the aforementioned distribution, while the one of the  $\alpha$  particle is a Gaussian with standard parameters [27]. The widely used potential  $v$  is given by the M3Y nucleon-nucleon interaction with Reid soft core parametrization [30–32] (see Ref. [2] for computational details).

The parameters of the M3Y interaction used to estimate the double-folding potential (2.10) were fixed by scattering experiments [30,31]. The resulting  $\alpha$ -core potential has a Woods-Saxon attractive plus Coulomb repulsive shape, but an  $\alpha$  particle can exist only on the nuclear surface, due to the strong Pauli suppression effects inside nucleus. A convenient way to simulate this situation is to match an harmonic oscillator repulsive core to the external part of the nuclear interaction procedure [33–35]. It makes use of the equality between the external attractive potential and internal repulsion and their first derivatives. This core fixes also the energy of the first resonant state to the experimental  $Q$  value,  $Q_\alpha$  [33,36]. Notice that the specific form of the repulsive core at small distances is irrelevant, due to the fact that the wave function vanishes here. Let us mention that the interval of the matched repulsion, simulating Pauli principle and fixing the  $Q$  value, is given until the second turning point, i.e.,  $R \in [0, R_2]$ . Therefore, the barrier between the second  $R_2$  and third turning points  $R_3$  has a realistic shape. As an example, for  $^{212}\text{Po} \rightarrow ^{208}\text{Pb} + \alpha$ ,  $R_2 \approx 8.9$  fm and  $R_3 \approx 29.5$  fm.

As we already mentioned, this interaction becomes axially deformed in the Henneberger system even for a spherical emitter. Therefore, the wave function of the  $\alpha$ -daughter system can be written as a multipole expansion,

$$\Psi_M(\mathbf{R}) = \sum_{L=0,2,4,\dots} \frac{f_L(R)}{R} Y_{LM}(\theta), \quad (2.11)$$

where the radial function  $f_L(R)$  describes the  $\alpha$ -daughter radial motion. The  $\alpha$ -daughter dynamics is described by the stationary Schrödinger equation

$$H\Psi_M(\mathbf{R}) = Q_\alpha \Psi_M(\mathbf{R}), \quad (2.12)$$

where  $Q_\alpha$  is relative energy of the emitted  $\alpha$  particle, called the  $Q$  value of the decay process. Because all measured decay widths are by many orders of magnitude smaller than the corresponding  $Q$  values, the stationarity approximation is a very good assumption. The Hamiltonian

$$H = -\frac{\hbar^2}{2\mu} \nabla_R^2 + V(\mathbf{R}) \quad (2.13)$$

is given by the kinetic operator, depending on the reduced mass  $\mu = m_N 4A_D / (4 + A_D)$ , plus the  $\alpha$ -core interaction,

which we split into spherical and axially deformed parts

$$\begin{aligned} V(\mathbf{R}) &= V_0(R) + V_d(\mathbf{R}) \\ &\equiv V_0(R) + \sum_{\lambda=2,4,\dots} V_\lambda(R) Y_{\lambda 0}(\theta). \end{aligned} \quad (2.14)$$

By using the orthonormality of the angular harmonics in the superposition (2.11), one obtains in a standard way the coupled system of differential equations for radial components [2]

$$\frac{d^2 f_L(R)}{d\rho^2} = \sum_{L'} A_{LL'}(R) f_{L'}(R), \quad (2.15)$$

where the coupling matrix is given by

$$\begin{aligned} A_{LL'}(R) &= \left[ \frac{L(L+1)}{\rho^2} + \frac{V_0(R)}{Q_\alpha} - 1 \right] \delta_{LL'} \\ &\quad + \frac{\langle Y_{L0} | V_d(\mathbf{R}) | Y_{L'0} \rangle}{Q_\alpha}, \end{aligned} \quad (2.16)$$

in terms of the reduced radius

$$\rho = \kappa R, \quad \kappa = \sqrt{\frac{2\mu Q_\alpha}{\hbar^2}}. \quad (2.17)$$

The matrix element of the interaction is given in terms of Clebsch-Gordan coefficients as follows:

$$\begin{aligned} &\langle Y_{L0} | V_d(\mathbf{R}) | Y_{L'0} \rangle \\ &= \sum_{\lambda=2,4,\dots} V_\lambda(R) \sqrt{\frac{(2L+1)(2L'+1)}{4\pi(2\lambda+1)}} (L0; L'0 | \lambda 0)^2. \end{aligned} \quad (2.18)$$

Let us mention that at large distances, where the field becomes spherical ( $V_d \rightarrow 0$ ) and purely Coulombian, the system of equations has a simple form:

$$\left[ -\frac{d^2}{d\rho^2} + \frac{L(L+1)}{\rho^2} + \frac{\chi}{\rho} - 1 \right] f_L(\chi, \rho) = 0. \quad (2.19)$$

The solution in each channel  $L$  has the following asymptotic expression:

$$f_L(\chi, \rho) \xrightarrow{R \rightarrow \infty} N_L H_L^{(+)}(\chi, \rho), \quad (2.20)$$

in terms of the outgoing Coulomb-Hankel spherical wave, depending on the Coulomb-Sommerfeld parameter

$$\chi = \frac{2Z_D Z_\alpha}{\hbar v} \sim \frac{2Z_D Z_\alpha}{\sqrt{Q_\alpha}}, \quad (2.21)$$

and reduced radius (2.17). Thus, a state which decays by  $\alpha$  emission is identified with a narrow resonant solution of the system of equations (2.15) that contains only outgoing components.

(a) The first step required in order to solve this system of equations is to define the internal and external fundamental solutions which satisfy the boundary conditions

$$\begin{aligned} \mathcal{R}_{LK}(R) &\xrightarrow{R \rightarrow 0} \delta_{LK} \varepsilon_c, \\ \mathcal{H}_{LK}^{(+)}(R) &\equiv \mathcal{G}_{LK}(R) + i\mathcal{F}_{LK}(R) \xrightarrow{R \rightarrow \infty} \delta_{LK} H_L^{(+)}(\kappa R) \\ &\equiv \delta_{LK} [G_L(\kappa R) + iF_L(\kappa R)], \end{aligned} \quad (2.22)$$

where  $\varepsilon_c$  are arbitrary small numbers. Here  $F_L(\chi, \rho)$  and  $G_L(\chi, \rho)$  are the standard regular and irregular spherical Coulomb functions. The index  $L$  labels the component while  $K$  indexes the solution.

(b) The second step is to build each component of the final solution as a superposition of  $N$  fundamental solutions. Imposing the matching conditions at a radius  $R_m$  inside the barrier, one obtains

$$f_L(R_m) = \sum_K \mathcal{R}_{LK}(R_m) M_K = \sum_K \mathcal{H}_{LK}^{(+)}(R_m) N_K,$$

$$\frac{df_L(R_m)}{dR} = \sum_K \frac{d\mathcal{R}_{LK}(R_m)}{dR} M_K = \sum_K \frac{d\mathcal{H}_{LK}^{(+)}(R_m)}{dR} N_K, \quad (2.23)$$

where the quantities  $N_K$ , multiplying Coulomb outgoing waves, are called scattering amplitudes.

(c) The third step is to find outgoing resonant states in this potential. Thus, the roots of the above homogeneous system of equations are given by the corresponding secular equation. They do not depend upon the matching radius  $R_m$ , because both internal and external solutions satisfy the same Schrödinger equation. The lowest root corresponds to the  $Q$  value of the  $\alpha$  decay between ground states. To obtain the unknown coefficients  $M_n$  and  $N_n$ , it is required to normalize the wave function in the internal region

$$\sum_L \int |f_L(R)|^2 dR = 1. \quad (2.24)$$

The angular distribution of emitted  $\alpha$  particles is given by the ratio

$$\Gamma(\theta)/\Gamma(0) = \lim_{R \rightarrow \infty} |\Psi_0(R, \theta)/\Psi_0(R, 0)|^2, \quad (2.25)$$

while the total decay width (integrated over the  $\alpha$ -emission angle  $\theta$ ) is the sum of partial components

$$\Gamma = \hbar v \sum_L N_L^2 \equiv \sum_L \Gamma_L, \quad v = \sqrt{\kappa/\mu}. \quad (2.26)$$

### III. NUMERICAL APPLICATION

In this section, we will analyze some important issues connected to the validity of the Kramers-Henneberger static approximation used in Ref. [16]: (1) which is the realistic  $\alpha$ -core interaction reproducing the measured half-lives in the absence of the laser field, instead of a simple sharp Coulomb barrier; (2) which is the influence of the time dependence induced by the standard Henneberger transformation on this interaction; and (3) which is the exact angular distribution of the emitted  $\alpha$  particles through a well-deformed realistic barrier, estimated within the exact coupled-channels procedure, instead of the simple WKB procedure.

We analyzed the  $\alpha$  clustering and emission from  $^{212}\text{Po}$  in a linearly polarized laser field, in order to answer the above listed three issues.

(1) As we already mentioned, the  $\alpha$  particle is born only at low nuclear densities, below 20% the equilibrium value (the so-called Mott  $\alpha$ -transition point), corresponding to the nuclear surface [25]. The realistic  $\alpha$ -core interaction reproducing this feature is given by the double-folding external

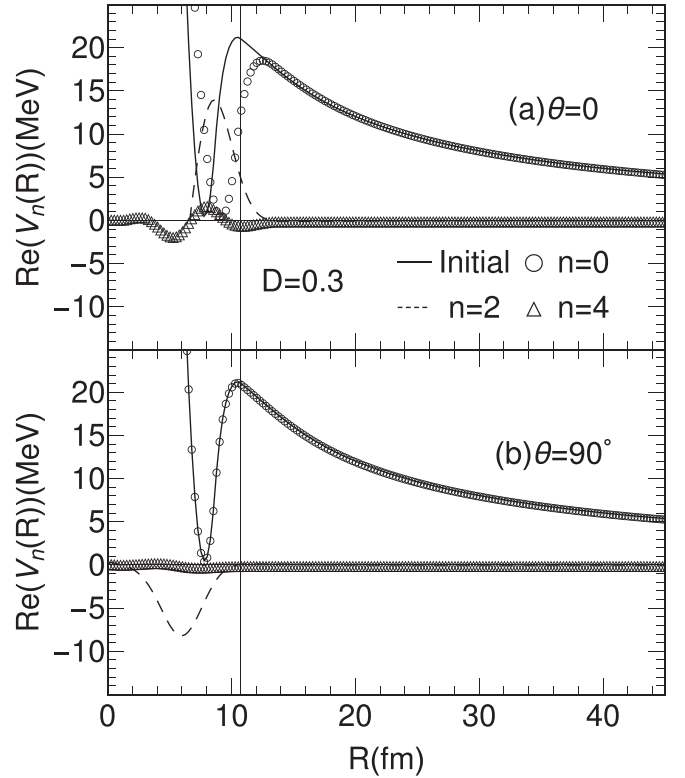


FIG. 1. Radial components of the Fourier transform (2.9) for  $D = S_0/R_N = 0.3$  corresponding to the decay process  $^{212}\text{Po} \rightarrow ^{208}\text{Pb} + \alpha$  for the real part at  $\theta = 0^\circ$  (a) and  $\theta = 90^\circ$  (b). The solid curve in all panels corresponds to the initial unperturbed potential. By a vertical line we indicated the maximum of the initial barrier.

Coulomb + nuclear parts [31], matched to an internal harmonic oscillator (ho) potential centered on the nuclear surface, simulating the Pauli suppression of the cluster inside nucleus. In Ref. [35], we have shown that such pocket-like interaction (Fig. 1 of this reference) is able to reproduce the experimental  $\alpha$ -decay half lives, by using a rather narrow interval of the ho length parameter  $b \in [0.6, 0.8]$  fm (Fig. 2 of this reference). Notice that in Ref. [25] this potential shape was confirmed by microscopic calculations for the binary system  $^{208}\text{Pb} + \alpha$ . Therefore, we investigated the influence of a monochromatic linearly polarized laser beam in the  $\theta = 0$  direction (2.6) on this realistic interaction in the Henneberger representation. We will keep unchanged the  $Q_\alpha$  value, as the first resonant state in the  $\alpha$ -daughter potential, because the laser frequency is by several orders of magnitude less than the experimental  $Q$  value.

(2) In Fig. 1, we plotted the Fourier amplitudes of the time-dependent pocket-like potential (2.9) in the Henneberger representation for  $D = S_0/R_N = 0.3$  versus radius. The real part of  $V_n(\mathbf{r})$  at  $\theta = 0$  is given in Fig. 1(a) and at  $\theta = 90^\circ$  in Fig. 1(b). Notice that the imaginary part of the Fourier spectrum vanishes. By a solid curve, we plotted in all panels the potential unperturbed by laser. Let us mention that the static  $n = 0$  component is by far dominant in the relevant region of the  $\alpha$ -particle penetration (barrier). The influence of  $n > 1$  components becomes important in the internal region,



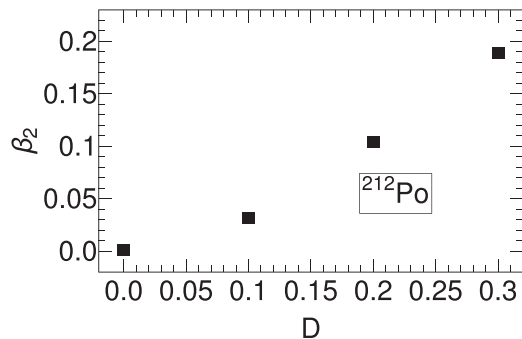


FIG. 2. Equivalent quadrupole deformation of the nuclear barrier vs  $D = S_0/R_N$  (2.8) for the decay process  $^{212}\text{Po} \rightarrow ^{208}\text{Pb} + \alpha$ .

where the  $\alpha$ -cluster formation is suppressed by the Pauli principle. The maximum for  $n > 0$  components at  $\theta = 0$  on the nuclear surface affects the  $\alpha$  formation in the pocket region of the potential. Intuitively, one can say the  $\alpha$ -cluster lives on the nuclear surface much longer than the period of the laser beam and it mainly “feels” the averaged (static) barrier before the penetration process. Notice that in atomic physics the Henneberger-Kramers static approximation is used in a different “adiabatic” context; namely, a particle moves in a rapidly changing potential, which can be “seen” as averaged during the process. In our case, the static component practically coincides with the initial external Coulomb barrier, except its top.

The Henneberger transformation allows for shifting all time dependence of the problem in the potential function. This transformation is unitary and perfectly allowed while allowing us to study the dynamics of the problem just from the potential point of view. In Fig. 1, it is readily observed that the outer barrier is affected only by the static component. Hence, the use of the *adiabatic* approximation in this region (as done in the Qi [20] and Pálffy papers [21]) is not justified. Beneath the nuclear surface, the higher Fourier components indeed do not vanish, but in this region the timescale is well defined as the time the nucleus spends before decaying. This interval can vary from a few  $\mu\text{s}$  to years, so the effective field can be averaged, canceling the oscillatory Fourier terms.

(3) The resulting static component of the potential in the Henneberger representation becomes deformed. Thus, in Fig. 2 we represented the equivalent quadrupole deformation of the nuclear surface corresponding to the barrier. We have shown that deformed nuclei, oriented in a strong magnetic field at very low temperatures, have a pronounced anisotropic  $\alpha$  emission toward the polar direction, where the Coulomb barrier becomes shorter [37]. In order to investigate a similar effect induced by a strong laser beam, shown in Fig. 1(a), we used the stationary coupled-channels method to integrate the Schrödinger equation. The  $\alpha$ -decaying state, describing emission between ground states, is the lowest Gamow resonance in the deformed potential with outgoing boundary conditions at a given experimental  $Q_\alpha$  value [2], which is not affected by the laser energy. In Fig. 3, we plotted the radial components of the wave function for increasing values of the parameter  $D$ .

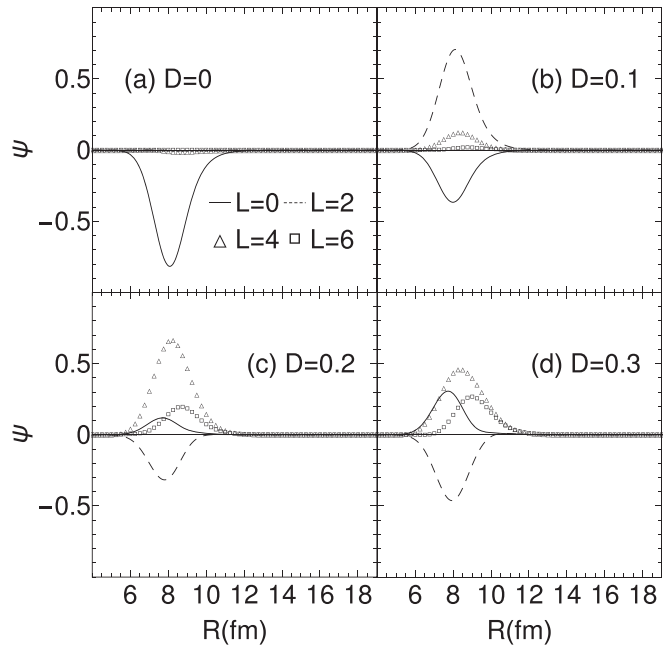


FIG. 3. Radial components of the wave function vs radius at different values of the parameter  $D = S_0/R_N$  (2.8) for the decay process  $^{212}\text{Po} \rightarrow ^{208}\text{Pb} + \alpha$ .

One remarks that all considered components become comparable by increasing  $D$ .

The occurrence of higher angular momentum components in the wave function is a general feature of axially deformed potentials. Since inside the nucleus the potential is strongly deformed (Figs. 1 and 2), it is expected that the ground-state wave function will also carry angular momenta higher than 0.

We then estimated the angular distribution according to Eq. (2.25). In Fig. 4, we plotted this quantity for the same values of the parameter  $D$ . As can be seen, the emission is indeed preferential in the polar direction, i.e., the same as the beam polarization, due to the small decrease of the barrier at  $\theta = 0$  in Fig. 1(a). As a rule, it strongly increases by increasing the parameter  $D$ , the ratio  $\Gamma(0)/\Gamma(90^\circ)$  reaching about four orders of magnitude at  $D = 0.3$ .

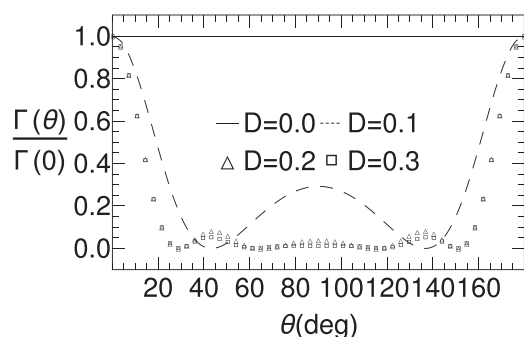


FIG. 4. Ratio  $\Gamma(\theta)/\Gamma(0)$  vs angle vs increasing values of the parameter  $D = S_0/R_N$  (2.7) for the decay process  $^{212}\text{Po} \rightarrow ^{208}\text{Pb} + \alpha$ .

#### IV. CONCLUSIONS

Concluding, a strong laser field deforms the realistic  $\alpha$ -daughter pocket-like interaction in the Henneberger representation and therefore the angular distribution of emitted particles and total decay width can be described only within the coupled-channels approach. Therefore, a spherical WKB approach for a constant nuclear  $\alpha$ -core attractive potential, surrounded by a sharp Coulomb barrier as used by some authors, is inadequate to describe  $\alpha$  emission in a strong laser field. Fourier analysis revealed that the static component is the most relevant in the region of the  $\alpha$ -particle formation and penetration, while time-dependent components have large

values inside the nucleus, where  $\alpha$ -cluster formation is hindered by the Pauli principle. Let us mention that this treatment is valid for an ideal monochromatic laser beam. In reality, the ratio of the laser signal to the interval between pulses is less than  $10^{-6}$  and therefore the analyzed effect is hindered. The predicted anisotropy is difficult to be evidenced by such short laser pulses and devices generating longer pulses are required.

#### ACKNOWLEDGMENT

This work has been supported by Grant No. PN-19060101/2019-2021 of the Romanian Ministry of Education and Research.

- 
- [1] A. M. Lane and R. G. Thomas, *Rev. Mod. Phys.* **30**, 257 (1958).  
 [2] D. S. Delion, *Theory of Particle and Cluster Emission* (Springer-Verlag, Berlin, 2010).  
 [3] P. Schuck, Y. Funaki, H. Horiuchi, G. Röpke, A. Tohsaki, and T. Yamada, *Phys. Scr.* **91**, 123001 (2016).  
 [4] D. S. Delion and A. Dumitrescu, *At. Data Nucl. Data Tables* **101**, 1 (2015).  
 [5] Extreme Light Infrastructure (ELI), [www.eli-laser.eu](http://www.eli-laser.eu).  
 [6] Extreme Light Infrastructure-Nuclear Physics (ELI-NP), [www.eli-np.ro](http://www.eli-np.ro).  
 [7] M. Y. Amusia and J. P. Connerade, *Rep. Prog. Phys.* **63**, 41 (2000).  
 [8] H. Schworer, J. Magill, and B. Beleites (eds.), *Lasers and Nuclei* (Springer-Verlag, Berlin, 2006).  
 [9] N. V. Zamfir, *Eur. Phys. J. Special Topics* **223**, 1221 (2014).  
 [10] G. D. Raikov, *Lett. Math. Phys.* **21**, 41 (1991).  
 [11] I. Gilary and N. Moiseyev, *Phys. Rev. A* **66**, 063415 (2002).  
 [12] A. M. Ishkhanyan and V. P. Krainov, *Laser Phys. Lett.* **12**, 046002 (2015).  
 [13] I. V. Kopytin and A. S. Kornev, *Phys. At. Nucl.* **77**, 53 (2014).  
 [14] Ș. Mișicu and M. Rizea, *J. Phys. G* **40**, 095101 (2013).  
 [15] Ș. Mișicu and M. Rizea, *Open Phys.* **14**, 81 (2016).  
 [16] D. S. Delion and S. A. Ghinescu, *Phys. Rev. Lett.* **119**, 202501 (2017).  
 [17] W. C. Henneberger, *Phys. Rev. Lett.* **21**, 838 (1968).  
 [18] M. Apostol, *Open Acc. J. Math. Theor. Phys.* **1**, 155 (2018).  
 [19] D. P. Kis and R. Szilvasi, *J. Phys. G* **45**, 045103 (2018).  
 [20] J. Qi, T. Li, R. Xu, L. Fu, and X. Wang, *Phys. Rev. C* **99**, 044610 (2019).  
 [21] A. Pálffy and S. Popruzhenko, [arXiv:1909.07826](https://arxiv.org/abs/1909.07826).  
 [22] D. Bai, D. Deng, and Z. Ren, *Nucl. Phys. A* **976**, 23 (2018).  
 [23] D. Bai and Z. Ren, *Commun Theor. Phys.* **70**, 559 (2018).  
 [24] P. Kalman, D. Kis, and T. Keszthelyi, *Phys. Rev. A* **87**, 063415 (2013).  
 [25] G. Röpke, P. Schuck, Y. Funaki, H. Horiuchi, Z. Ren, A. Tohsaki, C. Xu, T. Yamada, and B. Zhou, *Phys. Rev. C* **90**, 034304 (2014).  
 [26] H. Abele and G. Staudt, *Phys. Rev. C* **47**, 742 (1993).  
 [27] Dao T. Khoa, *Phys. Rev. C* **63**, 034007 (2001).  
 [28] R. Neu and F. Hoyer, *Phys. Rev. C* **46**, 208 (1992).  
 [29] M. Avrigeanu, A. C. Obreja, F. L. Roman, V. Avrigeanu, and W. von Oertzen, *At. Data Nucl. Data Tables* **95**, 501 (2009).  
 [30] G. Bertsch, J. Borysowicz, H. McManus, and W. G. Love, *Nucl. Phys. A* **284**, 399 (1977).  
 [31] G. R. Satchler and W. G. Love, *Phys. Rep.* **55**, 183 (1979).  
 [32] F. Cârstoiu and R. J. Lombard, *Ann. Phys. (NY)* **217**, 279 (1992).  
 [33] D. S. Delion, S. Peltonen, and J. Suhonen, *Phys. Rev. C* **73**, 014315 (2006).  
 [34] D. S. Delion, R. J. Liotta, and R. Wyss, *Phys. Rev. C* **92**, 051301(R) (2015).  
 [35] D. S. Delion, A. Dumitrescu, and V. V. Baran, *Phys. Rev. C* **97**, 064303 (2018).  
 [36] D. S. Delion and A. Sandulescu, *J. Phys. G* **28**, 617 (2002).  
 [37] D. S. Delion, A. Insolia, and R. J. Liotta, *Phys. Rev. C* **46**, 884 (1992).